Enhanced Binding of RNAP II CTD Phosphatase FCP1 to RAP74 Following CK2 Phosphorylation†

Karen L. Abbott,‡ Matthew B. Renfrow,§ Michael J. Chalmers,§ Bao D. Nguyen,‡,# Alan G. Marshall,§,|| Pascale Legault,*,‡ and James G. Omichinski*,‡,⊥

Department of Biochemistry and Molecular Biology and Department of Chemistry, University of Georgia, Athens, Georgia 30602, National High Magnetic Field Laboratory, Florida State University, 1800 East Paul Dirac Drive, Tallahassee, Florida 32310-4005, and Department of Chemistry, Florida State University, Tallahassee, Florida 32306

Received September 22, 2004; Revised Manuscript Received November 18, 2004

ABSTRACT: FCP1 (TFIIF-associated CTD phosphatase) is the first identified CTD-specific phosphatase required to recycle RNA polymerase II (RNAP II). FCP1 activity has been shown to be regulated by the general transcription factors TFIIF (RAP74) and TFIIB, protein kinase CK2 (CK2), and the HIV-1 transcriptional activator Tat. Phosphorylation of FCP1 by CK2 stimulates FCP1 phosphatase activity and enhances binding of RAP74 to FCP1. We have examined consensus CK2 phosphorylation sites (acidic residue $n + 3$ to serine or threonine residue) located immediately adjacent to both RAP74-binding sites of FCP1. We demonstrate that both of these consensus CK2 sites can be phosphorylated in vitro and that phosphorylation at either CK2 site results in enhanced binding of RAP74 to FCP1. The CK2 site adjacent to the RAP74-binding site in the central domain of FCP1 is phosphorylated at a single threonine site (T584). The CK2 site adjacent to the RAP74-binding site in the carboxyl-terminal domain can be phosphorylated at three successive serine residues (S942−S944), with phosphorylations at S942 and S944 both contributing to enhanced binding to RAP74. With the use of tandem Fourier transform−ion cyclotron resonance mass spectrometry (FT-ICR), we demonstrate that the phosphorylation of S942−S944 occurs in a semiordered fashion with the initial phosphorylation occurring at either S942 or S944 followed by a second phosphorylation to yield the S942/S944 diphosphorylated species. Using nuclear magnetic resonance (NMR) spectroscopy, we identify and map chemical shift changes onto the solution structure of the carboxyl-terminal domain of RAP74 ($RAP74_{436-517}$) on complexation of $RAP74_{436-517}$ with phosphorylated FCP1 peptides. These results provide new functional and structural information on the role of phosphorylation in the recognition of acidic-rich activation domains involved in transcriptional regulation, and bring insights into how CK2 and TFIIF regulate FCP1 function.

RNA polymerase II (RNAP II)[1] is a multi-subunit enzyme responsible for transcription of eukaryotic messenger RNA. The carboxyl-terminal domain (CTD) of the largest subunit of RNAP II contains a conserved repeat of the heptapeptide sequence (Y−S−P-T−S−P−S) (*1*, *2*). Phosphorylation and dephosphorylation at serine-2 and serine-5 within this repeat play an important role in regulating progression through the RNAP II transcription cycle (*3*, *4*). The hypophosphorylated form of RNAP II (RNAP IIA) is associated with the preinitiation complex (PIC), whereas the hyperphosphorylated form of RNAP II (RNAP IIO) is associated with the elongating RNAP II complexes (*5*, *6*). In addition to its role in passing from the initiation phase to the elongation phase of transcription, CTD phosphorylation has also been implicated in regulating post-transcriptional mRNA processing (*7*). Numerous kinases and phosphatases have been shown associate specifically with the CTD (*8*−*18*), and it is becoming increasingly clear that a complex regulatory network is required to maintain the precise phosphorylation state of the CTD.

† This work was supported by the National Institutes of Health Grant RO1 GM60298-01 (to J.G.O. and P.L.) and by NSF Grant CHE-99-09502 (A.G.M.), Florida State University, and the National High Magnetic Field Laboratory in Tallahassee, FL.

* Corresponding authors. Mailing and present address: Département de Biochimie, Université de Montréal, C.P. 6128, Succursale Centre-Ville, Montréal, QC, Canada H3C 3J7. Phone: (514) 343-7341. Fax: (514) 343-2210. E-mail: jg.omichinski@umontreal.ca; pascale.legault@umontreal.ca.

‡ Department of Biochemistry and Molecular Biology, University of Georgia.

§ National High Magnetic Field Laboratory, Florida State University.

|| Department of Chemistry, Florida State University.

⊥ Department of Chemistry, University of Georgia.

Present address: 164 Rowland Hall, University of California, Irvine, CA 92697-4675.

[1] Abbreviations: RNAP II, RNA polymerase II; CTD, carboxyl-terminal domain; PIC, preinitiation complex; FCP1, TFIIF-associated CTD phosphatase 1; TFIIF, general transcription factor IIF; hFCP1, human FCP1; yFCP1, yeast FCP1; BRCT, BRCA1-C-terminus; RAP74, RNA polymerase II-associated protein 74; TFIIB, general transcription factor IIB; CK2, protein kinase CK2; NMR, nuclear magnetic resonance; GST, glutathione s-transferase; GSH, glutathione (γ-glutamyl-cysteinyl-glycine); TFA, trifluoroacetic acid; HPLC, high performance liquid chromatography; MS, mass spectrometry; HEK, human embryonic kidney; ESI, electrospray ionization; FT-ICR, Fourier transform−ion cyclotron resonance mass spectrometry; SWIFT, stored waveform inverse Fourier transform; ECD, electron capture dissociation; AI-ECD, activated ion−electron capture dissociation; IRMPD, infrared multiphoton dissociation; HSQC, heteronuclear single quantum coherence; xFCP1, *Xenopus* FCP1.

10.1021/bi047958h CCC: $30.25
Published on Web 02/05/2005

FCP1 (TFIIF-associated CTD phosphatase 1) is a ubiquitous serine phosphatase with orthologs present in all eukaryotic species. FCP1 was the first RNAP II CTD-specific phosphatase identified (*14*−*18*), and it has been demonstrated to be a component of the mammalian RNAP II PIC (*16*, *19*). It has been proposed that one key function of FCP1 is to dephosphosphorylate the CTD of RNAP II, thus enabling the polymerase to undergo another transcription cycle (*18*, *19*). In addition, yeast capping enzymes Ceg1 and Abd1 are recruited to RNAP II via the phosphorylated CTD, and FCP1 phosphatase activity is essential for release of these capping enzymes (*20*). Besides its role in the recycling of RNAP II through its CTD phosphatase activity, FCP1 appears to serve other functions in regulating transcription. FCP1 functions as a positive regulator of transcription elongation, and this activity has been shown to be independent of its CTD phosphatase activity (*18*, *21*). Studies in yeast have established a genetic link between FCP1 and several transcriptional elongation factors (*21*−*23*). Furthermore, chromatin immunoprecipitation experiments demonstrate that FCP1 remains associated with the polymerase during elongation (*24*). Recently, a role for FCP1 in regulating mRNA processing has also been suggested although it is not clear if that function is associated with its phosphatase activity (*25*, *26*). FCP1 has been shown to co-immunoprecipitate with the methylosome complex (*27*), and FCP1 also associates with spliceosomal proteins (*27*).

FCP1 function is controlled by a number of nuclear factors that have been shown to interact with specific domains in FCP1. Human FCP1 (hFCP1) can be divided into three main domains based on sequence homology with yeast FCP1 (yFCP1) (*15*, *16*). The amino-terminal FCP1 homology domain (hFCP1 122−330) contains a conserved hydrophobic motif ΨΨΨDXDX(T/V)ΨΨ (where Ψ denotes hydrophobic residues) found in a family of small molecule phosphotransferases and phosphohydrolases (*18*, *19*, *28*). The central domain (hFCP1 544−728) contains a single BRCT (BRCA1 C-terminus) repeat, and yeast two-hybrid studies have revealed that this region of FCP1 is important for mediating interactions with the HIV-1 transcriptional activator Tat (*29*) and the large subunit of TFIIF (RAP74) (*16*, *29*). Binding of Tat and RAP74 to FCP1 may be mutually exclusive, since Tat can inhibit binding of RAP74 to this central domain of FCP1 (*29*). These interactions of Tat and TFIIF with the central domain of FCP1 may in part explain why Tat can inhibit FCP1 phosphatase activity in vitro (*30*), because RAP74 can stimulate FCP1 phosphatase activity (*31*). The CTD of FCP1 (hFCP1 812−961) is highly acidic. The amino acid composition of this domain is very similar to that found in acidic activation domains. In fact, FCP1 is capable of activating transcription both in vitro and in vivo when artificially recruited to a promoter (*19*, *32*). In addition, in vitro and in vivo binding studies have demonstrated that the carboxyl-terminal domain of FCP1 interacts with the carboxyl-terminal region of RAP74 and the first cyclin repeat of TFIIB (*16*, *31*, *33*). The FCP1-binding sites for both RAP74 and TFIIB consist of a shallow groove on the surface of the protein that is rich in both hydrophobic and basic amino acids (*34*). These interactions are believed to be responsible for the observation that TFIIF stimulates FCP1 phosphatase activity, whereas TFIIB inhibits the stimulation by TFIIF (*31*).

In addition to acting as a CTD phosphatase, FCP1 itself exists as a phosphoprotein (*35*, *36*) that copurifies with protein kinase CK2 (formerly known as casein kinase II) (*35*). These results suggest that CK2 could be an in vivo kinase for FCP1. In vitro studies examining the role of CK2 on FCP1 function demonstrated that phosphorylation of FCP1 by CK2 not only enhances RAP74 binding, but also stimulates CTD phosphatase activity (*35*, *36*). In contrast, elongation reactions conducted in the presence of CK2 are inhibited and this effect appears to be FCP1-specific, because CK2 added to elongation reactions in the absence of FCP1 had no effect (*35*). FCP1 is a highly acidic protein, and it contains several potential CK2 phosphorylation sites (*36*). The two RAP74-binding sites within FCP1 have been precisely mapped to highly conserved LXXLL-like acidic/hydrophobic motifs (*37*). The first RAP74-binding site is located within the central domain of FCP1 (*16*) (*29*), and the second is located in the carboxyl-terminal domain of FCP1 (*16*, *37*). Interestingly, both conserved RAP74-binding sites contain consensus CK2 phosphorylation sites (acidic residue $n + 3$ to serine or threonine residue) located immediately adjacent on the amino-terminal side. Given that CK2 phosphorylation enhances RAP74 binding to FCP1 (*36*), it is highly possible that phosphorylation of one or both of these CK2 sites located adjacent to the RAP74-binding sites may enhance RAP74 binding to FCP1.

In this manuscript, we further examine CK2 phosphorylation of FCP1. We identify consensus CK2 phosphorylation sites located immediately adjacent to both RAP74-binding sites of FCP1 that are highly conserved in all vertebrate FCP1 sequences. We demonstrate that both of these consensus CK2 sites can be phosphorylated in vitro and that phosphorylation at either the central or carboxyl-terminal CK2 site results in enhanced binding of RAP74 to FCP1. The CK2 site adjacent to the RAP74-binding site in the central domain is phosphorylated at a single threonine site (T584), whereas the CK2 site adjacent to the RAP74-binding site in the carboxyl-terminal domain is phosphorylated at three serine residues (S942, S943 and S944). With the use of tandem Fourier transform−ion cyclotron resonance (FT-ICR) mass spectrometry of synthetic peptide models of the carboxyl-terminal CK2 phosphorylyation site, we demonstrate that the phosphorylation of S942, S943 and S944 occurs in a semiordered fashion. The first phosphorylation occurs primarily at S942 or S944 followed by subsequent phosphorylation to yield a S942/S944 diphosphorylated species. Using nuclear magnetic resonance (NMR) spectroscopy, we identify chemical shift changes within residues of RAP74 following interaction with FCP1 peptides phosphorylated at T584, S942, and S944. In addition, we map these chemical shift changes on the solution structure of the carboxyl-terminal domain of RAP74 ($RAP74_{436-517}$). We discuss the functional and structural implications of CK2 phosphorylation on the regulation of FCP1.

EXPERIMENTAL PROCEDURES

Plasmids. The expression vectors for GST-$RAP74_{436-517}$ and GST-$FCP1_{879-961}$ have been described previously (*16*). The plasmid expressing the GST-$FCP1_{562-619}$ fragment used for in vitro binding studies was constructed by PCR amplification by use of pJA533 as a template (*16*). The

amplified FCP1 DNA fragment was digested with *BamH1* and *EcoR1* and then inserted in frame into the *BamH1* and *EcoR1* sites of the pGEX5X-1 GST-fusion expression vector (Amersham Biosciences, NJ). Clones expressing GST-$FCP1_{562-619}$ (T584E), GST-$FCP1_{879-961}$(S942A) and GST-$FCP1_{879-961}$ (S944A) were prepared by site-directed mutagenesis of the wild-type clones by use of the Quick Change kit (Stratagene, CA).

Antibodies. The RAP74 polyclonal antibody (C-18) and all secondary antibodies were purchased from Santa Cruz Biotechnologies (Santa Cruz, CA).

Purification of GST-FCP1 Fusion Proteins. GST-FCP1 fusion proteins were expressed in DH5α cells (Stratagene, CA). Cells were grown at 37 °C and protein expression was induced with 0.7 mM isopropyl-thiogalactoside (IPTG) for 3 h at 30 °C. The cells were harvested and resuspended in EBC buffer (50 mM Tris-HCl pH 8.0, 120 mM NaCl, 0.5% NP-40, and 2 mM DTT) supplemented with protease inhibitors (Sigma, MO): 1 μg/mL leupeptin, 2 μg/mL aprotinin, and 0.9 mg/mL PMSF. The cells were lysed by passage through a French press cell and centrifuged at 100000 x g for 40 min. The supernatant obtained from the high-speed centrifugation was added to glutathione (GSH)-sepharose resin (Amersham Biosciences, NJ) and incubated with mixing at 4 °C for 30 min. The resin was collected by centrifugation and washed four times with wash buffer (50 mM Tris-HCl pH 8.0, 100 mM NaCl, 1 mM EDTA, 0.5% NP-40, 0.05% SDS, and 1 mM DTT). GST-FCP1 fragments were eluted off the resin by incubation with 15 mM reduced GSH (Sigma, MO) for 10 min at 25 °C. The proteins were then dialyzed into storage buffer (50 mM Tris-HCl pH 8.0, 100 mM NaCl, 2 mM DTT, and 20% glycerol), and stored at −80 °C. The GST-FCP1 fragments were rebound to fresh GSH-sepharose resin prior to protein−protein binding studies.

Peptide Synthesis and Purification. Peptides $FCP1_{937-961}$, $FCP1_{937-961}$ ($S942PO_4$), and $FCP1_{937-961}$ ($S942PO_4$/$S944PO_4$) were purchased from the peptide synthesis facility at the Medical College of Georgia (Augusta, GA). The $FCP1_{579-600}$, $FCP1_{579-600}$ ($T584PO_4$), $FCP1_{941-961}$, and $FCP1_{584-607}$ peptides were synthesized by the solid-phase method with Fmoc chemistry using an Applied Biosystems (Foster City, CA) 430A peptide synthesizer. The $FCP1_{579-600}$, $FCP1_{579-600}$ (T584PO4) peptides were prepared with a glycine cap at the amino terminus. The phosphothreonine was incorporated as FmocThr(PO(OBzl)OH)-OH (Novabiochem, San Diego, CA). The $FCP1_{579-600}$ and $FCP1_{579-600}$ ($T584PO_4$) peptides were cleaved from the resin, and side-chain protecting groups were removed by incubation in reagent K (trifluoroacetic acid (TFA):phenol:thioanisole:H2O:ethanedithiol, 82.5:5:5:5:2.5) for 3 h at room temperature. All seven peptides were purified to homogeneity on a Vydac C_4 (Hesperia, CA) reversed-phase HPLC column (22 mm × 250 mm) with an acetonitrile gradient (30% to 50% over 20 min) in 0.05% TFA at a flow rate of 8 mL/min. The masses of peptides were confirmed by electrospray ionization mass spectrometry (MS).

Phosphorylation of Purified GST-FCP1 Fusion Proteins. Purified GST-FCP1 fusion proteins were first captured on 10 μL of GSH-sepharose resin. The resin-bound proteins were then diluted to a final protein concentration of 1 μM in 25 μL of CK2 reaction buffer [20 mM Tris-HCl pH = 7.5, 25 mM KCl, 10 mM $MgCl_2$, 350 μM ATP, 2.5 μCi [γ^{32}P]-ATP (for phosphorylation reactions without ^{32}P-ATP cold ATP was added at 0.5 mM)]. Phosphorylation reactions were initiated by the addition of 5 μL (10 units) protein kinase CK2 enzyme (NEB, MA) diluted in 20 mM Tris-HCl pH 7.5, 200 mM NaCl, 0.5 mM DTT, 10% glycerol, and 0.5% Triton X-100. The reactions were terminated by addition of SDS electrophoresis buffer, and the proteins were resolved on NuPage 12% gels in 1X MES electrophoresis buffer (Invitrogen, CA). ^{32}P-labeled GST-FCP1 fusion proteins were detected by PhosphorImager analysis (Molecular Dynamics, Amersham Pharmacia, NJ).

Phosphorylation of Purified Synthetic Peptides. For phosphorylation reactions, peptides (1 μM) and the appropriate controls (1 μM) were dissolved in the CK2 reaction buffer (25 μL final volume) described above. Phosphorylation reactions were initiated by the addition of 5 μL (10 units) protein kinase CK2 enzyme (NEB, MA) diluted in 20 mM Tris-HCl pH 7.5, 200 mM NaCl, 0.5 mM DTT, 10% glycerol, and 0.5% Triton X-100. The reactions were terminated by the addition of 1X SDS electrophoresis buffer, and phosphorylated peptides were resolved on 15% SDS polyacrylamide gels in 1X Tris-glycine buffer. ^{32}P-labeled peptides were detected by PhosphorImager analysis (Molecular Dynamics, Amersham Biosciences, NJ).

Protein−Protein Binding Assay. For binding reactions quantified and graphed, GST-$FCP1_{879-961}$, GST-$FCP1_{879-961}$ (S942A), and GST-$FCP1_{879-961}$ (S944A) were first purified on GSH-sepharose. The purified, resin-bound GST-FCP1 fusion proteins were then phosphorylated with CK2 prior to the binding studies. The CK2 phosphorylation reactions were performed at 25 °C from 0 to 60 min as described above, except the reactions were terminated by washing the resin twice with 20 mM Tris-HCl pH 8.0, 120 mM NaCl, 25 mM EDTA. Binding experiments were then performed at 4 °C for 1 h in 250 μL binding buffer (40 mM HEPES pH 8.0, 120 mM NaCl, 0.5% NP-40, 10 mM DTT). The binding experiment consisted of 1 μM of the CK2-treated resin-bound GST-FCP1 fusion proteins [GST-$FCP1_{879-961}$, GST-$FCP1_{879-961}$ (S942A), or GST-$FCP1_{879-961}$ (S944A)] and 1 μM of purified $RAP74_{436-517}$. The resin-bound protein−protein complexes were collected and washed three times in binding buffer. Proteins were resuspended in 1X SDS electrophoresis buffer and resolved on NuPage Bis-Tris 12% gels in 1X MES electrophoresis buffer (Invitrogen, CA) and transferred to Immobilon-P membrane (Millipore, MA). The bound RAP74 was detected by use of a 1:400 dilution of RAP74 (C-18) polyclonal antibody and a 1:10,000 dilution of an HRP-conjugated secondary antibody. Bound secondary antibodies were detected by chemiluminescence with the ECL-Plus kit (Amersham Biosciences, NJ). Bands were quantified by use of the Bio-Rad Versa Doc Imaging System. The membrane was stained subsequently with Coomassie blue to verify for equivalent GST-fusion protein input. Normalized values from three separate experiments were averaged and graphed in Figure 3.

Mass Spectrometry. Peptides were dissolved in 450 μL of CK2 reaction buffer described above. Phosphorylation reactions were initiated by the addition of 50 μL (100 units) protein kinase CK2 enzyme (NEB, MA) diluted in 20 mM Tris-HCl pH 7.5, 200 mM NaCl, 0.5 mM DTT, 10%

glycerol, and 0.5% Triton X-100 at 25 °C. After addition of the enzyme, the final peptide concentration was 0.3 mM. 25 μL samples were removed 1, 2, 4, 8, and 24 h after addition of the CK2 enzyme. The reactions were terminated by the addition of 25 μL of glacial acetic acid and lyophilized. In some cases, the phosphorylated peptides were resuspended in 25% aqueous acetic acid and resolved on a Vydac C_4 (Hesperia, CA) reversed-phase HPLC column (4.6 X 250 mm) with an acetonitrile gradient (30% to 50% over 20 min) in 0.05% TFA at a flow rate of 1 mL/min.

For the ESI experiments, samples from the peptide phosphorylation reactions were resuspended in 50 μL of water, and 10 μL of the stock solution was diluted to 50 μL in water. Prior to electrospray ionization (ESI), samples were desalted with a C_{18} ZipTip (Millipore, MA) into 30 μL of a 4:1 CH_3CN:H_2O solution containing 0.1−1% formic acid. Desalted samples were then microelectrosprayed from an emitter consisting of a 50 μm i.d. fused silica capillary that had been mechanically ground to a uniform thin-walled tip (*38*) at a flow rate of 200−400 nL/min.

The Fourier transform−ion cyclotron resonance (FT-ICR) MS experiments were performed with a home-built 9.4 T ESI Q FT-ICR mass spectrometer (*39*) under the control of a modular ICR data acquisition system (MIDAS) (*40*). Ions were transported through a Chait-style atmosphere-to-vacuum interface (*41*) and accumulated within a linear octopole ion trap, modified to allow improved ion ejection along the *z*-axis (*42*). Analyte ions were then transferred (1.0−1.4 ms) through an octopole ion guide to an open cylindrical ICR cell in which ions were captured by gated trapping. Ions were subjected to chirp (72−480 kHz at 150 Hz/μs) excitation (*43*, *44*) and direct-mode broadband detection (512 K time-domain data). Hanning apodization and one zero-fill were applied to all data prior to fast Fourier transformation and magnitude calculation (*45*). Frequency-domain spectra were calibrated (*46*) externally from the measured ICR frequencies of Agilent calibration mixture ions (*m*/*z* 622.02895, 922.00979, 1521.97146). Each displayed spectrum represents a sum of 1−50 time-domain transients. Masses and *m*/*z* values were calculated with Isopro 3.1 (MS/MS software, http://members.aol.com/msmssoft/).

For FT-ICR MS/MS experiments, precursor ions were mass-selectively accumulated externally for 20−40 s (*47*). Following transfer to the ICR cell (1.0 ms), stored-waveform inverse Fourier transform (SWIFT) (*48*, *49*) ejection was applied for higher-resolution isolation of the peptide ion of interest. The instrumental configuration and experimental parameters for electron capture detection (ECD), infrared multiphoton dissociation (IRMPD), and activated ion electron capture dissociation (AI-ECD) are described in detail elsewhere (*39*).

For IRMPD, precursor ions were irradiated with a 40 W, 10.6 μm, CO_2 laser (no beam expander, Synrad, Mukilteo, WA), Photon irradiation was for 100 ms at 35% laser power (14 W). For ECD, precursor ion populations were irradiated with low energy electrons for 10 ms. For activated ion A I-ECD, precursor ion isolation and electron irradiation were performed as described above. Following electron irradiation, ions were irradiated with the IR laser for 100 ms at 10−20% laser power (4−8 W). Following MS/MS (ECD, IRMPD, or AI-ECD), product ions were subjected to chirp excitation (58 to 480 kHz at 150 Hz/μs) and direct-mode broadband detection (512 K time-domain data). Each displayed spectrum represents the sum of 50−60 time domain transients.

Phosphate Group Modifications. β-Elimination/Michael addition reactions were carried out with a modified version of the procedure described by Shen et al. (*50*). 3.7 μL (5 μg) of $FCP1_{937\text{-}961}$ peptide solution following phosphorylation was combined with 13 μL H_2O, 9 μL 1-propanol, 3 μL of 200 mM $Ba(OH)_2$, and 1.3 μL ethanethiol to yield final concentrations of 30% (v/v) 1-propanol, 20 mM $Ba(OH)_2$, and 0.5 M ethanethiol. The solution was then incubated at 45 °C for between 0.5 and 5 h and the reaction was terminated by the addition of 15 μL of 1 M ammonium sulfate to form a barium sulfate salt. The barium sulfate was then removed by centrifugation at 10000 × *g* for 5 min, and the supernatant was desalted and electrosprayed as described above.

NMR Spectroscopy. The ^{15}N-labeled $RAP74_{436-517}$ was expressed from a pGEX-2T vector (Amersham Biosciences, NJ) in BL21(DE3). Labeled protein was obtained by growth in a modified minimal medium containing ^{15}N-labeled NH_4Cl as the sole source of nitrogen as previously described (*34*). NMR samples of the complexes were prepared by addition in four equal increments of the appropriate peptide to ^{15}N-labeled $RAP74_{436-517}$ to obtain the final 1:1 complex. The final NMR sample consisted of 0.20 mM ^{15}N-labeled $RAP74_{436-517}$ and 0.20 mM FCP1 peptides ($FCP1_{579-600}$, $FCP1_{579-600}$ ($T584PO_4$), $FCP1_{937-961}$, $FCP1_{937-961}$ ($S942PO_4$) or $FCP1_{937-961}$ ($S942PO_4$/$S944PO_4$) in 500 μL of 20 mM sodium phosphate pH 6.5 and 1 mM EDTA (90% H_2O/ 10% D_2O). The 2D ^{1}H-^{15}N HSQC spectra (*51*) were collected at 27 °C with a Varian Unity Inova 600 MHz NMR spectrometer equipped with a z pulsed-field gradient unit and an HCN triple resonance probe. The NMR data were processed with NMRPipe/NMRDraw (*52*) and ribbon diagrams were generated by the program MOLMOL (*53*).

Model of the $FCP1_{879-961}$ ($S942PO_4$/$S944PO_4$)/$RAP74_{436-517}$ Complex. Three-dimensional structures of the $FCP1_{879-961}$ ($S942PO_4$/$S944PO_4$)/$RAP74_{436-517}$ were calculated with the Torsion Angle Molecular Dynamics protocol of CNS, starting from two extended structures (one for RAP74 residues 451−517) and one for FCP1 residues 879−961) with standard geometry and modified phosphoserine (FCP1 residues 942 and 944). Structure calculation was performed with the same NMR-drived restraints and protocol used for the structure determination of the $FCP1_{879-961}$/$RAP74_{436-517}$ complex (*37*). To model the potential ionic bridges between K475 and $S942PO_4$ and between K480 and $S944PO_4$ two constraints were added between K475 H_ζ (protons) and $S942PO_4$ OP (oxygens of the phosphate group) and between K480 H_ζ (protons) and $S944PO_4$ OP (oxygens of the phosphate group). These restraints were added on the basis of observed NMR chemical shift changes. These restraints are set from 1.8 to 2.5 Å^2 with a force constant of 75 kcal/mol, as used for the other NOE restraints. A set of 50 structures was calculated, and the 20 structures with lowest energies were chosen for further evaluation and for determination of the average minimized structure. These structures had no NOE violation greater than 0.2 Å and no dihedral angle (φ and ψ) violation greater than 5°.

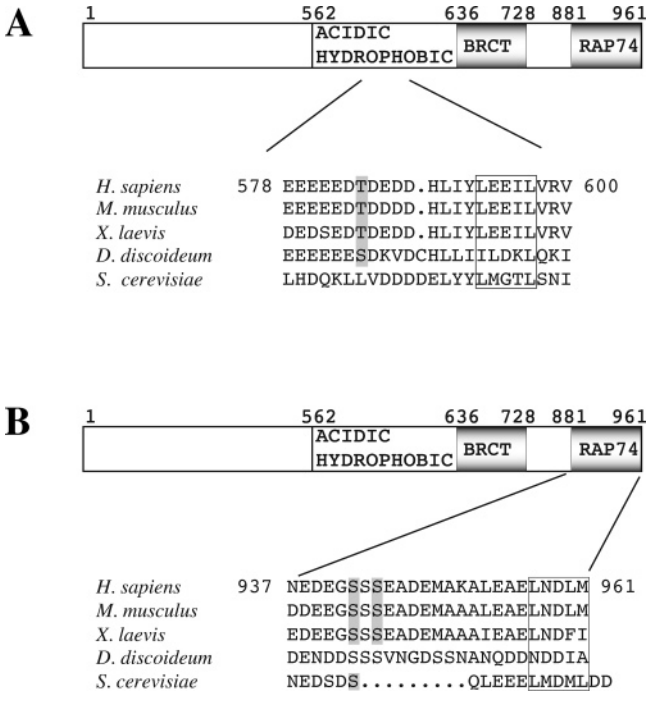

FIGURE 1: Amino acid sequence of FCP1 highlighting the CK2 phosphorylation sites adjacent to the two RAP74-binding sites in FCP1. Sequences from the **(**A**)** central domain and **(**B**)** carboxyl-terminal domain of FCP1 from *Homo sapiens* (NP_004706), *Mus musculus* (AAH53435), *Xenopus laevis* (Q98SN2), *Dictyostelium discoideum* (AAM33170), and *Saccharomyces cerevisiae* (NP_014004) were aligned by use of BLAST (Altschul et al. 1990) followed by manual refinement. The conserved small hydrophobic motif required for RAP74 binding is boxed, and the predicted sites of CK2 phosphorylation based on presence of an acidic residue at the $n + 3$ position are highlighted (*54*).

RESULTS

CK2 Phosphorylation Sites in FCP1 Located Adjacent to RAP74-Binding Sites. Previous experiments have demonstrated that both *Xenopus* FCP1 (xFCP1) isolated from *Xenopus* A6 cells (*36*) and human FCP1 isolated from baculovirus-infected SF9 cells exist as phosphoproteins (*35*). In addition, phosphorylation of xFCP1 by CK2 leads to enhanced binding of xFCP1 to xRAP74 in vitro, and it is believed that this enhanced binding to RAP74 may be crucial for FCP1 function (*36*). However, the exact mechanism by which CK2 phosphorylation of FCP1 leads to enhanced binding to RAP74 is unknown. There are two known RAP74-binding sites in FCP1 and either or both of these two sites could be responsible for the enhanced binding observed after phosphorylation of FCP1 by CK2 (*15*, *16*, *29*, *33*, 36). The first RAP74-binding site is located in the central domain of FCP1 on the amino-terminal side of the BRCT domain (Figure 1A, residues 579−600) (*29*), and the second RAP74-binding site is located at the extreme carboxyl terminus of FCP1 (Figure 1B, residues 937−961). Interestingly, both RAP74-binding sites in FCP1 are located immediately adjacent to consensus CK2 phosphorylation sites (*54*), and these predicted CK2 phosphorylation sites (acidic residue $n + 3$ to serine or threonine residue) are highly conserved in many species with higher conservation in vertebrates (highlighted in Figure 1A and Figure 1B). The central domain contains a threonine CK2 phosphorylation site (T584), whereas the carboxyl-terminal domain contains two serine CK2 phosphorylation sites (S942 and S944). Our initial goal was to determine if the predicted CK2 sites at either the central domain or the carboxyl-terminal domain could be phosphorylated by CK2 in vitro and if phosphorylation at these sites by CK2 resulted in enhanced binding of FCP1 to RAP74.

CK2 Phosphorylation of T584 Enhances RAP74 Binding to FCP1 In Vitro. As mentioned above, the central domain of FCP1 contains a highly conserved consensus CK2 phosphorylation site (acidic residue $n + 3$ to serine) (*54*), and in hFCP1 the predicted site of phosphorylation is at amino acid T584 (Figure 2A). To determine if the central domain of FCP1 could be phosphorylated in vitro by CK2 at T584, equimolar concentrations (1 μM) of casein, GST, GST-FCP1$_{562-619}$, or GST-FCP1$_{562-619}$ (T584E) were incubated for 30 min with recombinant CK2 in the presence of [γ-^{32}P]-ATP. Following the phosphorylation reaction with CK2, the various proteins were checked for incorporation of the ^{32}P label (Figure 2B). It is clear that both the control casein and GST-FCP1$_{562-619}$ were phosphorylated by CK2 in vitro, but that GST and GST-FCP1$_{562-619}$ (T584E) were not phosphorylated to any significant degree. Based on these experimental results (Figure 2B), we conclude that CK2 is capable of phosphorylating GST-FCP1$_{562-619}$ specifically at residue T584 in vitro and that T584 is the primary CK2 phosphorylation site within the central domain in vitro.

Since CK2 is capable of phosphorylating GST-FCP1$_{562-619}$ at T584 in vitro, we attempted to determine if phosphorylation at T584 led to enhanced binding of RAP74 to FCP1$_{562-619}$. Resin-bound GST and GST-FCP1$_{562-619}$ were first treated for 30 min with either a mock CK2 phosphorylation reaction (all components except enzyme) or a CK2 phosphorylation reaction. Following these treatments, the resin-bound GST and GST-FCP1$_{562-619}$ were used in binding reactions with purified RAP74$_{436-517}$ (Figure 2C). RAP74 binding to FCP1 was determined by Western blot detection with a polyclonal antibody against RAP74. In these experiments, RAP74$_{436-517}$ was able to bind to either GST-FCP1$_{562-619}$ treated with the mock reaction (Figure 2C, lane 4) or to GST-FCP1$_{562-619}$ treated with the CK2 reaction (Figure 2C, lane 5). However, the CK2-treated GST-FCP1$_{562-619}$ displays enhanced binding to RAP74$_{436-517}$ relative to the mock-treated GST-FCP1$_{562-619}$. As expected, RAP74$_{436-517}$ did not bind to either the GST mock or GST CK2 reaction (Figure 2C, lanes 2 and 3, respectively).

CK2 Phosphorylation of S942 and S944 Enhances RAP74 Binding to FCP1 In Vitro. Like the central domain, the RAP74-binding domain at the extreme carboxyl terminus of FCP1 is also located adjacent to a CK2 phosphorylation site. The consensus CK2 site at the carboxyl terminus contains three consecutive serine residues (S942−S944) sandwiched between numerous acidic amino acids (Figure 2A). It is predicted that both S942 and S944 should be ideal targets for CK2 phosphorylation (acidic residue $n + 3$ to serine) (*54*). To determine if the carboxyl-terminal domain of FCP1 could be phosphorylated in vitro by CK2, equimolar concentrations (1 μM) of casein, GST, GST-FCP1$_{879-961}$, GST-FCP1$_{879-961}$ (S942A), and GST-FCP1$_{879-961}$ (S944A) (Figure 2D) were incubated for 10 and 30 min with recombinant CK2 in the presence of [γ-^{32}P]-ATP. Following the phosphorylation reaction with CK2, the various proteins were checked for incorporation of the ^{32}P label (Figure 2D). It is

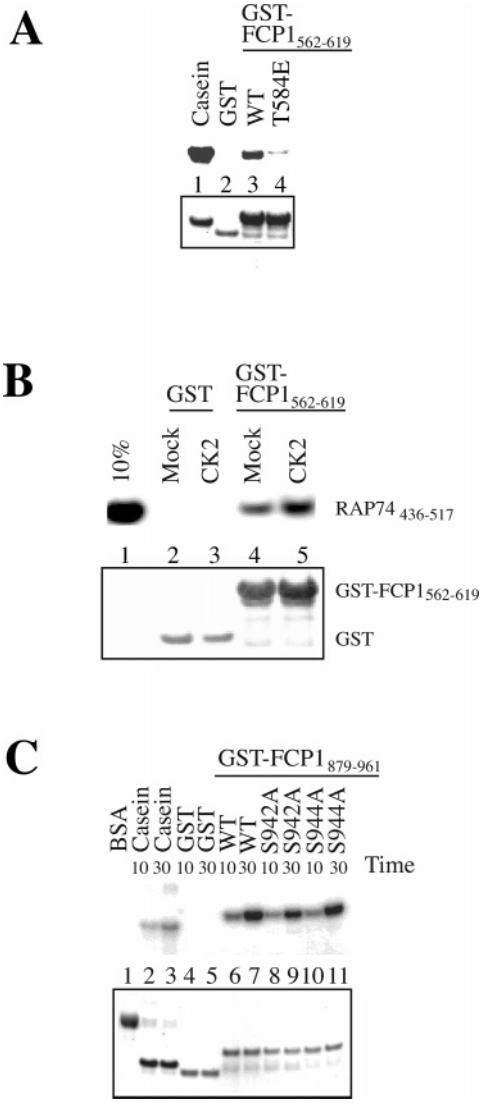

FIGURE 2: Identification of CK2 phosphorylation sites in the FCP1 central and carboxyl-terminal domains in vitro by ^{32}P labeling. **(**A**)** Phosphorylation of 1) casein 2) GST 3) GST-FCP1$_{562-619}$ (WT) and 4) GST-FCP1$_{562-619}$ (T584E) mutant in the presence of [$\gamma-^{32}$P]-ATP (4500 Ci/mmol) and recombinant CK2. Each reaction contained approximately 25 μg protein input; the ^{32}P-labeled proteins were detected by PhosphorImager analysis. **(**B**)** Captured GST (lanes 2−3) or GST-FCP1$_{562-619}$ (lanes 4−5) proteins were mock-phosphorylated (all components except enzyme; lanes 2 and 4) or CK2-phosphorylated (lanes 3 and 5), as described in materials and methods. Each binding reaction contained GST (2 μM) or GST-FCP1$_{562-619}$ (2 μM) and RAP74$_{436-517}$ (10 μM). The bound RAP74$_{436-517}$ protein was detected with the RAP74 polyclonal antibody (C-18). 10% input of RAP74$_{436-517}$ is shown as a control (lane 1). **(**C**)** Phosphorylation of casein (lanes 2−3), GST (lanes 4−5), GST-FCP1$_{879-961}$ (WT) (lanes 6−7), GST-FCP1$_{879-961}$ (S942A) (lanes 8−9), or GST-FCP1$_{879-961}$ (S944A) (lanes 10−11) for 10 or 30 min in the presence of [γ-^{32}P]-ATP (4500 Ci/mmol) and recombinant CK2. Each reaction contained approximately 25 μg protein input; the ^{32}P-labeled proteins were detected by PhosphorImager analysis. 10% input of RAP74$_{436-517}$ is shown as a control (lane 1). For **(**A**)**, (B) and (C**)** equivalent input of GST and GST-FCP1 fusion protein was verified by Coomassie-blue staining of the membrane (boxed).

clear that CK2 is capable of phosphorylating GST-FCP1$_{879-961}$, GST-FCP1$_{879-961}$ (S942A), and GST-FCP1$_{879-961}$ (S944A), and they all appear to be phosphorylated to similar extents. There are two plausible explanations for these results. The first explanation is that both S942 and S944 are phosphorylated by CK2 in vitro as predicted. The second explanation is that CK2 is phosphorylating the carboxyl-terminal region of FCP1 at residues other than either S942 or S944.

Since CK2 is capable of phosphorylating FCP1$_{879-961}$ in vitro, we attempted to determine if this phosphorylation led to enhanced binding of RAP74 to FCP1$_{879-961}$. Resin-bound GST and GST-FCP1$_{879-961}$ were first treated for 30 min with either a mock CK2 phosphorylation reaction or a CK2 phosphorylation reaction. Following the treatments, the resin-bound GST and GST-FCP1$_{879-961}$ were used in binding reactions with purified RAP74$_{436-517}$ (Figure 3A). As before, RAP74 binding was determined by Western blot detection with a polyclonal antibody against RAP74. RAP74$_{436-517}$ bound to both FCP1$_{879-961}$ treated with the mock reaction (Figure 3A, lane 4) and to FCP1$_{879-961}$ treated with the CK2 reaction (Figure 3A, lane 5), but the CK2-treated FCP1$_{879-961}$ displays enhanced binding to RAP74$_{436-517}$ relative to the mock-treated FCP1$_{879-961}$. RAP74$_{436-517}$ did not bind to either the GST mock or GST CK2 reaction (Figure 3A, lanes 2 and 3, respectively).

Since S942 and S944 are CK2 phosphorylation sites and they are located immediately adjacent to the carboxyl-terminal RAP74-binding site in FCP1, we tested if the S942A or S944A mutations would have any effect on the enhanced binding of FCP1$_{879-961}$ to RAP74 following CK2 phosphorylation. First, purified GST-FCP1$_{879-961}$, GST-FCP1$_{879-961}$ (S942A), and GST-FCP1$_{879-961}$ (S944A) were bound to GSH−Sepharose. The resin-bound proteins were then incubated for 0, 10, and 60 min with recombinant CK2. Following the CK2 treatment, the resin-bound GST-FCP1$_{879-961}$, GST-FCP1$_{879-961}$ (S942A), and GST-FCP1$_{879-961}$ (S944A) proteins were used in binding reactions with purified RAP74$_{436-517}$ (Figure 3B). Surprisingly, both the S942A mutation and the S944A mutation caused a reduction in the enhanced binding of FCP1$_{879-961}$ to RAP74 following CK2 phosphorylation. These results in combination with the previously described phosphorylation studies suggest that phosphorylation at both S942 and S944 contributes to the enhanced binding of RAP74 to the carboxyl-terminal domain of FCP1 (FCP1$_{879-961}$) and maximum binding is observed only when both S942 and S944 are phosphorylated.

Synthetic Peptide Models Containing T584, S942, and S944 Are Phosphorylated by CK2. To further demonstrate that T584, S942, and S944 of FCP1 can be phosphorylated by CK2, we prepared a series of synthetic peptides for phosphorylation experiments in vitro (Figure 3C). In the initial experiments, the peptides were incubated with recombinant CK2 in the presence of [γ-^{32}P]-ATP, and the phosphorylation reaction was monitored by checking for incorporation of the ^{32}P label as described above for the longer FCP1 fragments. We tested four synthetic peptides as potential CK2 substrates corresponding to FCP1$_{937-961}$, FCP1$_{579-600}$, FCP1$_{941-961}$, and FCP1$_{584-607}$ (Figure 3C). Interestingly, the peptides corresponding to FCP1$_{937-961}$ and FCP1$_{579-600}$ are phosphorylated in vitro by CK2, but the peptides corresponding to FCP1$_{941-961}$ and FCP1$_{584-607}$ are not. These results were also supported by HPLC analysis of the incubations, where we failed to see any new species formed in the presence of CK2 with FCP1$_{579-600}$ and FCP1$_{941-961}$ (data not shown). The current explanation for these observations are that the phosphorylation sites are located too close to the amino-terminal end of the peptide.

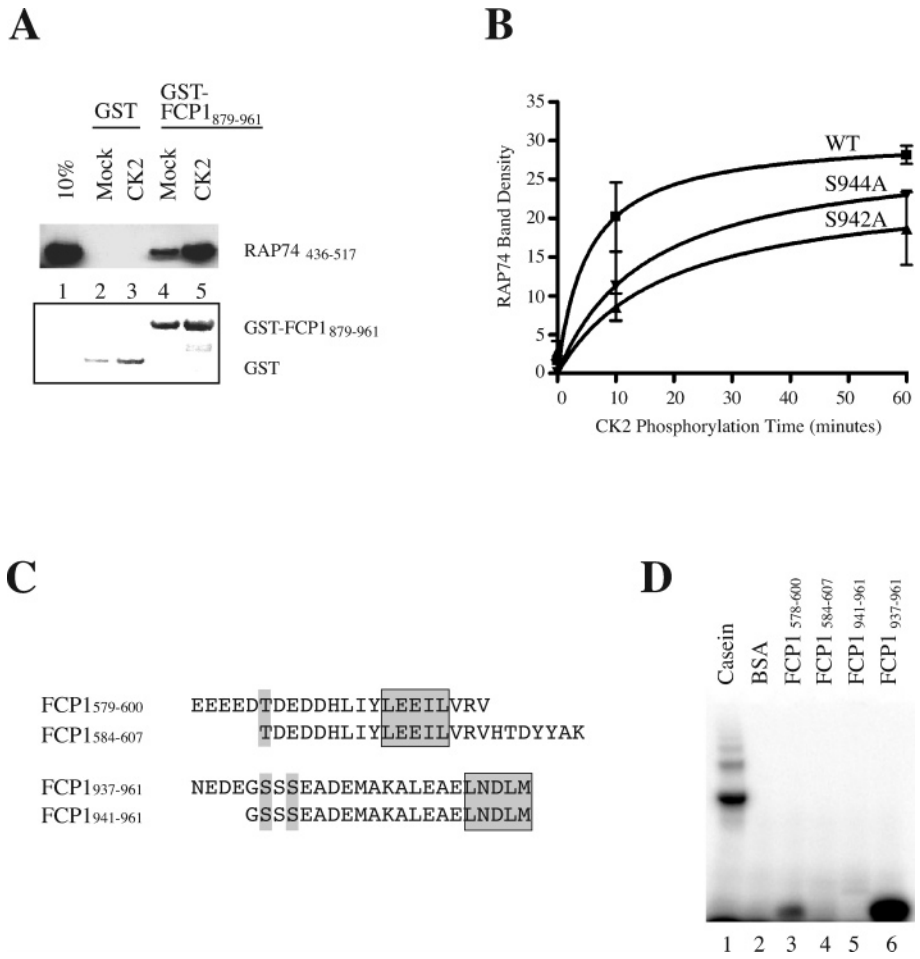

FIGURE 3: S942 and S944 within the carboxyl-terminus of FCP1 are phosphorylated by CK2 in vitro and mediate enhanced RAP74 binding. **(**A**)** Binding reaction of resin bound GST (lanes 2−3) and GST-FCP1$_{879-961}$ (lanes 4−5) mock-phosphorylated (all components except enzyme; lanes 2 and 4) and CK2-phosphorylated (lanes 3 and 5) with RAP74$_{436-517}$ as described in material and methods. Each binding reaction contained GST (2 μM) or GST-FCP1$_{879-961}$ (2 μM) and purified RAP74$_{436-517}$ (10 μM). The boundRAP74$_{436-517}$ protein was detected with the RAP74 polyclonal antibody (C-18). 10% input of RAP74$_{436-517}$ is shown as a control (lane 1). Equivalent input of GST and GST-FCP1 fusion protein was verified by Coomassie-blue staining of the membrane (boxed). **(**B**)** Graphical representation of the enhancement in RAP74 binding after 0, 10, and 60 min of CK2 phosphorylation reactions with wild-type (WT) GST-FCP1$_{879-961}$ (■), GST-FCP1$_{879-961}$ (S942A) (▲), and GST-FCP1$_{879-961}$ (S944A) (▼). CK2 phosphorylation reactions were stopped by the addition of 100 mM EDTA followed by washing in binding buffer 2−3 times. Concentrations of binding reactions are the same as described for **(**A**)**. RAP74 binding is expressed as measured band density on ECL Hyperfilm (Amersham Biosciences, NJ) scanned on a Bio-Rad Fluor S Multi-Imager (Bio-Rad, CA). Data shown is averaged data from three separate experiments with error bars. **(**C**)** The synthetic peptides FCP1$_{579-600}$, FCP1$_{584-607}$, FCP$_{937-961}$ and FCP1$_{941-961}$ used for in vitro CK2 phosphorylation reactions. The location of the CK2 sites (shaded) and small hydrophobic motifs (boxed and shaded) are highlighted. **(**D**)** Casein (lane 1), BSA (lane 2), FCP1$_{579-600}$ (lane 3), FCP1$_{584-607}$ (lane 4), FCP$_{941-961}$ (lane 5), and FCP$_{937-961}$ (lane 6) were incubated for 30 min in the presence of [γ-^{32}P]-ATP (4500 Ci/mMol) and recombinant CK2. Each reaction contained 25 μg of protein input and the ^{32}P-labeled proteins were detected by PhosphorImager analysis.

S942, S943, and S944 Are Phosphorylated by CK2 in a Semiordered Fashion. Next, we used the synthetic peptide corresponding to FCP1$_{937-961}$ to demonstrate that both S942 and S944 can be phosphorylated by CK2 in vitro and to determine if there was a preference for phosphorylation at S942 or S944. The FCP1$_{937-961}$ peptide was incubated with recombinant CK2 for varying periods of time (0−48 h) followed by addition of acetic acid to terminate the reaction. The reactions were then analyzed by HPLC to verify the presence of phosphorylated peptides. The HPLC analysis (data not shown) showed that following the addition of CK2, a large percentage (~70%) of the peptide was converted into two new species within the first 2 h. Longer incubations (21−48 h) with CK2 resulted in a third new species. Our initial hypothesis was that the first two new species corresponded to mono-phosporylated FCP1$_{937-961}$ and diphosphorylated FCP1$_{937-961}$, whereas the third new species corresponded to the triphosphorylated FCP1$_{937-961}$ peptide.

To verify this hypothesis and to determine which serines were phosphorylated in the FCP1$_{937-961}$ peptide, we performed tandem FT-ICR mass spectrometry (MS/MS) experiments. Following incubation with CK2 for 0−4 h, both IRMPD and ECD FT-ICR MS/MS analysis were performed on the CK2-treated FCP1$_{937-961}$ peptide at various time points. IRMPD FT-ICR MS/MS of the mono-phosphorylated peptide showed significant loss of H_3PO_4 from precursor and phosphorylated product ions, however, a sufficient number of product ions with phosphorylation indicated the site of phosphorylation was S942. ECD fragmentation allows peptide bonds to broken into sequence specific *c* and *z*$^{\bullet}$ ions with little or no loss of labile post-translational modifications (*39*). Figure 4 shows the mass spectrum obtained following

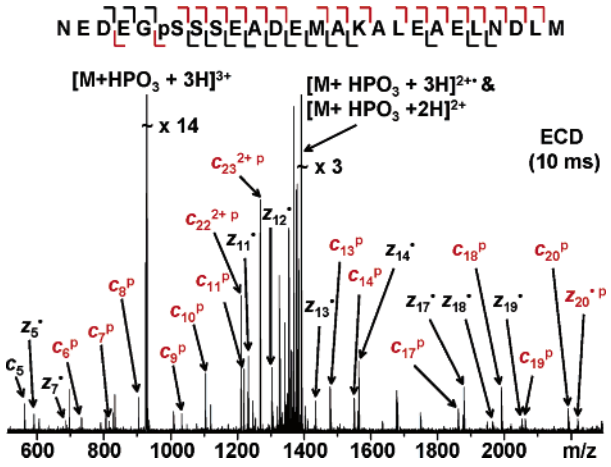

FIGURE 4: ESIFT-ICR mass spectrum following ECD of $FCP1_{937-961}$ synthetic peptide after 4 h CK2 phosphorylation reaction. This product ion spectrum was obtained from population of quadrupole- and SWIFT-isolated $[N_{937}EDEGSSSSEADEMAKALEAELNDLM_{961} + HPO_3 + 3H]^{3+}$ FCP1 peptide precursor ions. Twenty-one (out of twenty-four) peptide backbone bonds are broken. The location of the phosphorylation site is identified by the observation of the $[c_6 + HPO_3]^+$ ions, as well as the $[z^{\bullet}_{19}]^+$, $[z^{\bullet}_{19}]^+$, $[z^{\bullet}_{20} + HPO_3]^+$, and $[z^{\bullet}_{22} + HPO_3]^+$, ions.

ECD of the mono-phosphorylated peptide ($[N_{937}EDEGSSSEADEMAKALEAELNDLM_{961} + HPO_3 + 3H]^{3+}$ ions after 10 ms electron irradiation (sum of 50 time-domain transients). The detection of the $[c_6 + HPO_3]^+$ ions, combined with the detection of $[c_7 + HPO_3]^+$ and $[c_8 + HPO_3]^+$ ions, indicates that the site of phosphorylation is at serine 942 (Figure 5, top). That conclusion is corroborated by the detection of the $[z_{18}]^+$ and $[z_{19}]^+$ ions (without HPO_3) and $[z_{20} + HPO_3]^+$ ion, again identifying the predominant site of mono-phosphorylation as serine 942 (Figure 5, bottom). Although we can confirm HPO_3 attachment at S942, low signal-to-noise ratios of the $[c_6 + HPO_3]^+$ (Figure 5, top), $[z_{20} + HPO_3]^+$ ions, $[z_{18}]^+$ ions, and $[z_{19}]^+$ ions (without HPO_3, Figure 5, bottom) do not allow us to eliminate the possibility of lower abundance species with mono-phosphorylation at S943 or S944.

Although the initial ESI FT-ICR mass spectrum of the CK2-treated $FCP1_{937-961}$ peptide demonstrated the presence of the nonphosphorylated and mono-phosphorylated peptide, HPLC analysis of an equivalent sample indicated the presence of additional species that we attributed to di- and triphosphorylated $FCP1_{937-961}$ peptides. Our inability to detect the presence of either di- or triphosphorylated $FCP1_{937-961}$ peptides as positive ions could be due to their low electrospray ionization efficiencies during positive-ion ESI.

To further investigate the presence of the di- and triphosphorylated peptide species, we utilized a method described by Shen et al. (*50*, *55*). In this method, the charged phosphate groups are removed by β-elimination and replaced by the Michael addition of ethanethiol. This modification results in a decrease in the acidity of the solution phase ion, and therefore increased efficiency of electrospray generation of peptide positive ions (when compared to the native phosphopeptide). Indeed, ESI FT-ICR MS analysis of derivatized $FCP1_{937-961}$ peptide following incubation with CK2 for 4 h reveals the presence of both the di- and triphosphorylated $FCP1_{937-961}$ peptide (Figure 6).

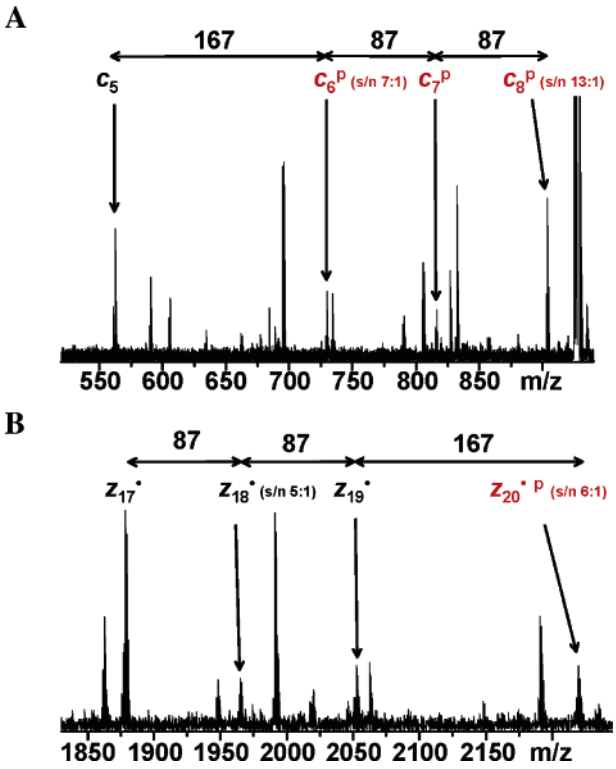

FIGURE 5: Mass scale expanded segments of the ECD FT-ICR MS/MS spectrum in Figure 4 showing the c_5-c_8 (top) and $z^{\bullet}_{17}$–$z^{\bullet}_{20}$ (bottom) fragment ion series. The fragment ion series from both the amino-terminal (c ions) and carboxyl-terminal ($z^{\bullet}$ ions) ends of the mono-phosphorylated $FCP1_{937-961}$ peptide demonstrate the predominant site of attachment to be S942 (see text).

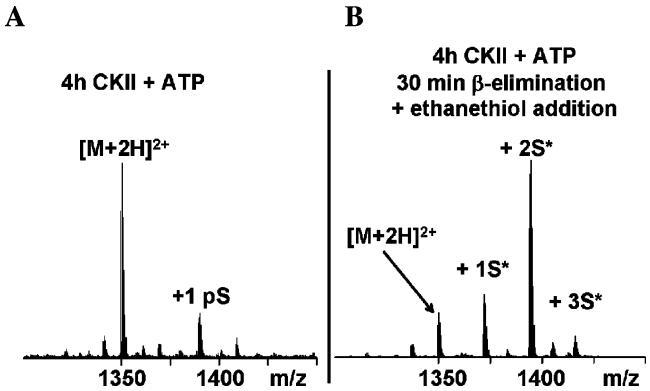

FIGURE 6: β-Elimination/ethanethiol modification of phosphorylated $FCP1_{937-961}$ peptide increases the positive ion mode electrospray ionization efficiency of multiply phosphorylated FCP1 ions. Left: Segment of the positive-ion ESI FT-ICR MS spectrum of the phosphorylated (4 h CK2 phosphorylation reaction) $FCP1_{937-961}$ fragment. $[M + 2H]^{2+}$ and $[M + HPO_3 + 2H]^{2+}$ ions are detected with good signal/noise ratios, but no ions corresponding to di- or triphosphorylated $FCP1_{937-961}$ are detected. Right: Positive-ion ESI FT-ICR MS spectrum of an equivalent amount of $FCP1_{937-961}$ fragment after 30 min β-elimination and Michael addition. S-Ethylcysteine modified peptide ions (e.g. + S*) confirm the presence of the di- and triphosphorylated forms of the $FCP1_{937-961}$ peptide.

Once the presence of the di- and triphosphorylated $FCP1_{937-961}$ peptides was established, tandem MS could be used to identify the specific sites phosphorylated in the diphosphorylated peptides. This distinction was possible because the mass of the dephosphorylated and modified serine residue is unique among all common amino acids (except methionine), and the sequence of the peptide is known. The

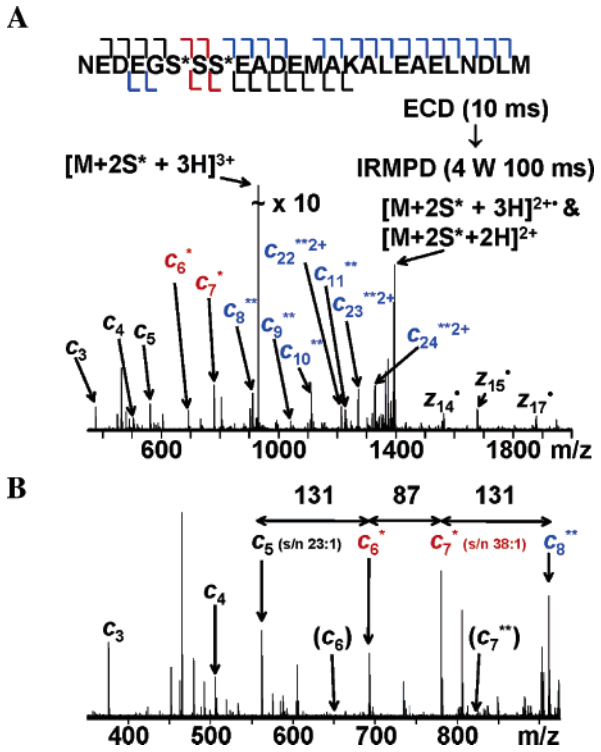

FIGURE 7: ESI FT-ICR MS/MS spectrum of the S-ethylcysteine modified $FCP1_{937-961}$ fragment. Top: Product ion spectrum obtained from AI-ECD FT-ICR MS/MS of a population of quadrupole- and SWIFT-isolated $[N_{937}EDEGSSSSEADEMAKALEAELNDLM_{961} + 2S^* + 3H]^{3+}$ $FCP1_{937-961}$ precursor ions. Twenty-three (out of twenty-four) peptide backbone bonds are broken. Bottom: Sites of modification are identified by the observation of c_6* and c_8** ions and the absence of c_6 and c_7** ions (in parentheses).

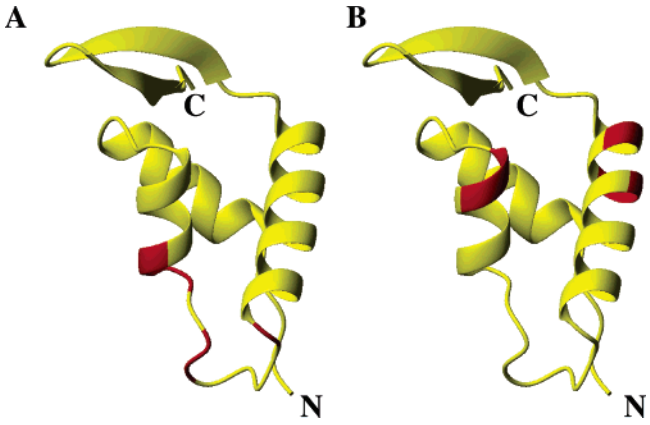

FIGURE 8: Changes in NMR chemical shifts of $RAP74_{436-517}$ residues on complexation with phosphorylated FCP1 binding sites. Ribbon diagram of the NMR structure of $RAP74_{436-517}$ with mapping of the signals that undergo a significant chemical shift change ($\Delta\delta > 0.07$ ppm; $\Delta\delta = [(0.17\Delta N_H)^2 + (\Delta H_N)^2]^{1/2}$) upon comparison of the 2D ^1H-^{15}N HSQC spectra from **(A)** the $RAP74_{436-517}/FCP1_{937-961}$ complex with the $RAP74_{436-517}/FCP1_{937-961}$ ($S942PO_4/S944PO_4$) complex and **(B)** the $RAP74_{436-517}$ /$FCP1_{579-600}$ complex with the $RAP74_{436-517}/FCP1_{579-600}$ ($T584PO_4$) complex. The signals are mapped onto the NMR structure of $RAP74_{436-517}$ (yellow) and the locations of significantly shifted signals are indicated in red.

mass spectrum obtained following AI-ECD of $(N_{937}EDEGSSSEADEMAKALEAELNDLM_{961} + 2(C_2H_6S) + 3H)^{3+}$ demonstrates that S942 and S944 are specifically modified and not S943 (Figure 7A and 7B), based on a 131 Da mass difference between the c_5-c_6 and c_7-c_8, versus an 87 Da (mass of an unmodified serine residue) between the c_6 and c_7 ions. If the CK2 phosphorylations of $FCP1_{937-961}$ peptide were nonspecific, the precursor ion population could be comprised of a heterogeneous mixture of diphosphorylated $FCP1_{937-961}$ peptide ions (942* + 943*, 943* + 944*, or 942* + 944*). Although these isobaric peptides could not be distinguished based on mass alone, tandem mass spectrometry allows us to determine if the precursor ion population is homogeneous or not. The results (Figure 7B) indicate that the first site of phosphorylation is predominantly at S942, followed by subsequent phosphorylation to yield the diphosphorylated species at both S942 and S944, and finally by phosphorylation at S943 to give the triphosphorylated species.

Mapping the Binding Site of $S942PO_4$ and $S944PO_4$ onto the Structure of $RAP74_{436-517}$. To map the interaction site for the two phosphorylated serines that contribute to enhanced RAP74 binding in the carboxyl-terminal of FCP1 ($S942PO_4$ and $S944PO_4$) onto the solution structure of $RAP74_{436-517}$, we recorded 2D $^1H-^{15}N$ HSQC spectra of three complexes: $FCP1_{937-961}/^{15}N$-labeled $RAP74_{436-517}$, $FCP1_{937-961}$ ($S942PO_4$)/^{15}N-labeled $RAP74_{436-517}$, and $FCP1_{937-961}$ ($S942PO_4/S944PO_4$)/^{15}N-labeled $RAP74_{436-517}$. As expected, the 2D ^1H-^{15}N HSQC spectrum of $FCP1_{937-961}$ bound to ^{15}N-labeled $RAP74_{436-517}$ is virtually identical to that previously reported for $FCP1_{879-961}$ bound to ^{15}N-labeled $RAP74_{436-517}$ (*34*) (data not shown). To identify the binding site for both $S942PO_4$ and $S944PO_4$ from FCP1 on the solution structure of $RAP74_{436-517}$, we first computed the differences in ^1H and ^{15}N chemical shifts between the $RAP74_{436-517}/FCP1_{937-961}$ complex and the $RAP74_{436-517}/FCP1_{937-961}$ ($S942PO_4/S944PO_4$) complex. Six out of 82 amino acid residues of $RAP74_{436-517}$ displayed significant chemical shift differences ($\Delta\delta > 0.07$ ppm; $\Delta\delta = [(0.17\Delta N_H)^2 + (\Delta H_N)^2]^{1/2}$) between the two complexes. These residues correspond to K475, K476, F477, T479, K480, and S485 of $RAP74_{436-517}$. When these residues are mapped onto the NMR solution structure of $RAP74_{436-517}$ (Figure 8A), we see that the region near the end of helix H2 and the beginning of helix H3, and the flexible loop (L2) that connects H2 to H3 appear to be crucial for the binding of $S942PO_4$ and the $S944PO_4$. Interestingly, this area is extremely rich in lysine residues (K475, K476, K480, K481), and thus it is possible that several of these lysine residues form an ion pair with either $S942PO_4$ or $S944PO_4$. In fact, three of these lysine residues (K475, K476, and K480) displayed significant changes in chemical shifts upon formation of the complex with the diphosphorylated peptide.

In an attempt to specifically identify the lysine residues that interact with either the $S942PO_4$ or the $S944PO_4$, we then computed the differences in ^1H and ^{15}N chemical shifts between the $RAP74_{436-517}/FCP1_{937-961}$ complex and the $RAP74_{436-517}/FCP1_{937-961}$ ($S942PO_4$) complex. This analysis reveals that 5 out of 82 amino acid residues of $RAP74_{436-517}$ displayed significant changes ($\Delta\delta > 0.07$ ppm; $\Delta\delta = [(0.17\Delta N_H)^2 + (\Delta H_N)^2]^{1/2}$) between the two complexes. These residues correspond to positions K475, K476, F477, T479, and S485 of $RAP74_{436-517}$. We then computed the differences in ^1H and ^{15}N chemical shifts of the $RAP74_{436-517}/FCP1_{937-961}$ ($S942PO_4$) complex and the $RAP74_{436-517}/FCP1_{937-961}$ ($S942PO_4/S944PO_4$) complex. None of the residues of $RAP74_{436-517}$ displayed significant differences

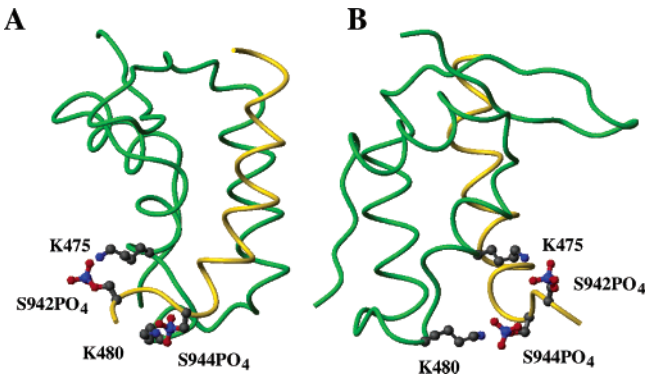

FIGURE 9: Model of the interactions between $RAP74_{436-517}$ and $FCP1_{937-961}$ ($S942PO_4$/$S944PO_4$). Models were generated from the NMR structure and constraints of the $RAP74_{436-517}$/$FCP1_{879-961}$ complex as a starting point. In the models, the serines at position 942 and 944 of FCP1 were substituted with phosphoserines and constraints were added for the interactions between the lysines of RAP74 and the phosphoserines as described in materials and methods (A) Backbone trace of the $RAP74_{436-517}$ (green)/$FCP1_{937-961}$ ($S942PO_4$/$S944PO_4$) (gold) model complex highlighting the interactions between the lysine amino acids of $RAP74_{436-517}$ (K475/K480) and the phosphoserine residues of $FCP1_{937-961}$ ($S942PO_4$/$S944PO_4$) at the interface. **(B)** This model is a 90° rotation of **(**A**)**.

($\Delta\delta > 0.07$ ppm; $\Delta\delta = [(0.17\Delta N_H)^2 + (\Delta H_N)^2]^{1/2}$ between the complexes containing the mono-phosphorylated and the diphosphorylated peptides. However, we did observe that two amino acid residues of $RAP74_{436-517}$ displayed intermediate chemical shift changes (0.07 ppm $< \Delta\delta > 0.04$ ppm; $\Delta\delta = [(0.17\Delta N_H)^2 + (\Delta H_N)^2]^{1/2}$) between the two complexes, and these residues correspond to K476 and K480 of $RAP74_{436-517}$. Based on these results, we postulate that $S942PO_4$ makes an ion pair with K475 of RAP74, whereas $S944PO_4$ makes an ion pair with K476 and/or K480 of RAP74, and both these interactions likely contribute to enhanced binding of FCP1 to RAP74.

$K475/S942PO_4$ and $K480/S944PO_4$ Ion Pairs in the $RAP74_{436-517}$/$FCP1_{879-961}$ Complex. Analysis of our NMR structure of the $RAP74_{436-517}$/$FCP1_{879-961}$ complex verified that K475 was the closest lysine residue of RAP74 to S942 of FCP1 at a distance of 13 Å, whereas K480 is the closest lysine of RAP74 to S944 of FCP1 at 18 Å. Although these distances are too large for an ion pair, the S942 and S944 are located in an extremely flexible portion of $FCP1_{879-961}$ and K480 is located in the highly flexible L2 loop of $RAP74_{436-517}$. Thus, it is highly conceivable that there is enough mobility to make ion pairs between these lysines and the phosphorylated serines. To demonstrate that these two ion pairs are in fact possible, we modeled them into the existing NMR structure of the $RAP74_{436-517}$/$FCP1_{879-961}$ complex. In the modeling calculations, S942 and S944 were replaced with $S942PO_4$ and $S944PO_4$. In addition, we included a distance constraint of 2.5 Å between the side chain H_ζ protons of K475 and the oxygens attached to phosphorus of $S942PO_4$, and a distance constraint of 2.5 Å between the side chain H_ζ protons of K480 and the oxygens attached to phosphorus of $S944PO_4$. In these modeling calculations, all structural constraints, including the two new distant constraints, were not violated, and the resulting structure demonstrated the feasibility of the $K475/S942PO_4$, and the $K480/S944PO_4$ ion pairs (Figure 9).

Mapping the Binding Site of $T584PO_4$ onto the Structure of $RAP74_{436-517}$. To map the interaction site for the phosphorylated threonine in the central domain of FCP1 ($T584PO_4$) onto the solution structure of $RAP74_{436-517}$, we computed the differences in ^1H and ^{15}N chemical shifts between the $RAP74_{436-517}$/$FCP1_{579-600}$ complex and the $RAP74_{436-517}$/$FCP1_{578-600}$ ($T584PO_4$) complex. This analysis reveals that 2 out of 82 amino acid residues of $RAP74_{436-517}$ displayed significant chemical shift differences ($\Delta\delta > 0.07$ ppm; $\Delta\delta = [(0.17\Delta N_H)^2 + (\Delta H_N)^2]^{1/2}$) between the complexes. These residues correspond to positions T470 and K498 of $RAP74_{436-517}$. In addition, we observe 3 other amino acid residues of $RAP74_{436-517}$ that displayed intermediate chemical shift changes (0.07 ppm $< \Delta\delta > 0.04$ ppm; $\Delta\delta = [(0.17\Delta N_H)^2 + (\Delta H_N)^2]^{1/2}$) between the two complexes. These residues correspond to K471, Q495 and I496 of $RAP74_{436-517}$. When mapped onto the NMR solution structure of $RAP74_{436-517}$, we see that T470 and K471 are located at the beginning of the H2 helix, and residues Q495, I496 and K498 are located at the end of the H3 helix (Figure 8B). These two points are located on the opposite side of the hydrophobic groove. Based on these results and analysis of the NMR structure of the $RAP74_{436-517}$/$FCP1_{879-961}$ complex, we postulate that $T584PO_4$ could either make an ion pair with K471, a hydrogen bond with T470, or both. Although the chemical shift data suggests a possible involvement of K498 this possibility appears unlikely based on homology with the structure of the $RAP74_{436-517}$/$FCP1_{879-961}$ complex. The chemical shift changes at Q495, I496 and K498 most likely result from of a rearrangement of the hydrophobic groove between the H2 and H3 helices of $RAP74_{436-517}$ to accommodate the $FCP1_{578-600}$ ($T584PO_4$) peptide. We are currently determining the NMR structure of the $RAP74_{436-517}$/$FCP1_{579-600}$ ($T584PO_4$) complex to better define the role of the $T584PO_4$.

DISCUSSION

In this manuscript, we examine the role of phosphorylation of human FCP1 by CK2. FCP1 contains numerous potential CK2 phosphorylation sites, and previous studies have clearly shown that CK2 is capable of phosphorylating FCP1 in vitro (*35*, *36*). In an earlier study, it was shown that xFCP1 exists as a phosphoprotein and copurifies with CK2 (*36*). It was also demonstrated that phosphorylation of xFCP1 by CK2 enhances binding to RAP74, leading to a stimulation of FCP1 CTD phosphatase activity. Furthermore, a serine to alanine mutation at residue 457 in xFCP1 lowers overall phosphorylation of xFCP1 and leads to a significant inhibition of CK2-enhanced FCP1 CTD phosphatase activity. Although these studies established a clear role for S457 in CK2 enhancement of FCP1 CTD phosphatase activity, the CK2 phosphorylation site in FCP1 responsible for the increased RAP74 binding was not identified. Furthermore, S457 is not contained within either of the two previously identified RAP74-binding sites of FCP1, and therefore it is unlikely that its phosphorylation would enhance binding of RAP74 to FCP1. In the second study, human FCP1 isolated from baculovirus was also shown to exist in a phosphorylated state, and CK2 was isolated as an FCP1-specific kinase from HeLa cell nuclear extracts (*35*). In addition, TFIIF (RAP30/RAP74) was shown to be capable of activating the CTD phosphatase activity of the phosphorylated form of FCP1, but not the

unphosphorylated form, and the phosphorylated form of FCP1 was shown to be more active in stimulating transcription elongation reactions then the unphosphorylated form. Interestingly, elongation reactions conducted in the presence of CK2 were inhibited. This inhibitory effect was FCP1-specific, since CK2 added to elongation reactions in the absence of FCP1 displayed no such inhibitory effect. In addition, human FCP1 isolated from the baculovirus system was shown to be phosphorylated at S575 and S740 by mass spectral analysis. However, it was not determined if CK2 or an alternative kinase was responsible for phosphorylating these serine residues, and it is not known if phosphorylation of these sites has an important role in either enhancing FCP1 CTD phosphatase activity or enhancing FCP1 binding to RAP74.

T584 is in the central domain of FCP1, and is located within the FCP1-binding site for both Tat and RAP74 (*29*). Phosphorylation of T584 could potentially play an important role in regulating FCP1 activities associated with RAP74 and Tat interactions. T584 is surrounded by acidic amino acids, with acidic amino acids located at $n-4$, $n-3$, $n-2$, $n-1$, $n+1$, $n+2$, $n+3$ and $n+4$ (Figure 1A) suggesting it is an ideal site for CK2 phosphorylation. We have demonstrated that CK2 is capable of phosphorylating FCP1 specifically at residue T584 in vitro and that T584 is the predominant CK2 phosphorylation site within the central domain of GST-$FCP1_{562-619}$. In addition, phosphorylation of T584 by CK2 leads to enhanced binding of $FCP1_{562-619}$ to $RAP74_{436-517}$. Preliminary NMR studies with a $RAP74_{436-517}$/$FCP1_{579-600}$ ($T584PO_4$) complex indicate that this enhanced binding appears to be the result of $T584PO_4$ making a salt bridge and/or hydrogen bond with the H2 helix of $RAP74_{436-517}$. The hydrogen bond would form with residue T470 of $RAP74_{436-517}$, whereas the salt bridge would be with K471 of $RAP74_{436-517}$. $FCP1_{879-961}$ contains a motif in the last 22 amino acids that resembles the motif found in $FCP1_{579-600}$. In fact, it is possible to align the LXXLL-like hydrophobic motif found in $FCP1_{579-600}$ (L593−L597), with the LXXLL-like acidic/hydrophobic motif found in $FCP1_{879-961}$ (L957−M961). When the two motifs are aligned, D583 aligns with D947 and $T584PO_4$ aligns with E948 (Figure 2A). In the NMR structure of the $FCP1_{879-961}$/$RAP74_{436-517}$ complex, D947 of FCP1 makes a salt bridge with K471 of RAP74, and E954 of FCP1 makes a hydrogen bond with T470 of RAP74, whereas E948 of FCP1 is exposed to the solvent. If the positioning of the FCP1 helix in the $RAP74_{436-517}$/$FCP1_{879-961}$ and $RAP74_{436-517}$/$FCP1_{579-600}$ ($T584PO_4$) complexes were identical, then $T584PO_4$ would be solvent exposed and would not be able to enhance the binding of FCP1 to RAP74. Our hypothesis is that the helix formed by $FCP1_{579-600}$ ($T584PO_4$) when complexed with $RAP74_{436-517}$ is shorter and more flexible at the amino terminus then the helix formed by FCP1 in the $FCP1_{879-961}$/$RAP74_{436-517}$ complex allowing for $T584PO_4$ to make a salt bridge with K471. In addition, repositioning of the ion pair may be required to allow the bulkier hydrophobic aromatic residue (Y592) present in $FCP1_{579-600}$ ($T584PO_4$) to be positioned in the hydrophobic groove of $RAP74_{436-517}$. There are no aromatic amino acids in $FCP1_{879-961}$.

Based on these studies, it appears that S575 is not a major phosphorylation target for CK2 in vitro and it is difficult to structurally explain how phosphorylation at this site could result in enhanced binding to RAP74. It is clear that this residue is phosphorylated when FCP1 is expressed in baculovirus (*35*). However it does not appear that this phosphorylation is carried out by CK2 unless the in vivo conditions in baculovirus with the full-length FCP1 are significantly different than our in vitro conditions with $FCP1_{562-619}$. S575 is surrounded by acidic residues at $n-2$, $n+2$, $n+3$, $n+4$, $n+5$, $n+6$, and $n+7$, and there is a crucial acidic residue at the $n+3$ position. Therefore, under the simplest definition, S575 meets the minimal requirements to be considered a potential CK2 site. However, it is also clear from our results, in which we fail to see phosphorylation of the $FCP1_{941-961}$ and $FCP1_{584-607}$ peptides (Figure 3D), that other factors are very important for the CK2 phosphorylation site selection in addition an acidic residue at position $n+3$.

S942, S943, and S944 are located in the carboxyl-terminal domain of FCP1, and this domain has been previously shown to be important for interaction with RAP74 and TFIIB (*15*, *16*, *31*, *33*, *34*). We have demonstrated that S942, S943, and S944 can be phosphorylated by CK2 in vitro and that phosphorylation of both S942 and S944 is required for maximum binding of FCP1 ($FCP1_{879-961}$) to $RAP74_{436-517}$ following phosphorylation with CK2. Tandem FT-ICR mass spectral analysis of a $FCP1_{937-961}$ peptide revealed that the three phosphorylations occur in a semiordered fashion. We do not observe a mixed population of diphosphorylated peptides, but instead phosphorylation of only S942 and S944 and not S943. Furthermore, NMR analysis clearly indicates that when $FCP1_{879-961}$ is complexed to $RAP74_{436-517}$, both $S942PO_4$ and $S944PO_4$ are in position to interact with lysine residues in $RAP74_{436-517}$. Based on changes in chemical shift mapping, analysis of the NMR structure of the $RAP74_{436-517}$/$FCP1_{879-961}$ complex, and modeling, we postulate that $S942PO_4$ makes a salt bridge with K475 of $RAP74_{436-517}$, and $S944PO_4$ makes a salt bridge with K480 of $RAP74_{436-517}$. It should be emphasized that the affected region of RAP74 is rich in lysine residues (K475, K476, K480, K481) and the loop between the H2 and H3 helices is highly flexible. Thus, it is highly possible that all four lysines are important for the enhanced binding of FCP1 following phosphorylation either through formation of direct ion pairs or simply through electrostatic effects.

Although a detailed kinetic analysis was not performed, it appears that following the initial phosphorylation primarily at S942 (Figures 4 and 5), there is a rapid phosphorylation at the alternative position (S944 and S942) (Figures 6 and 7), and finally slower phosphorylation at S943. Successive phosphorylations have been observed in several other CK2 sites containing multiple serine residues, but there is currently no detailed analysis of the order of phosphorylation in these multi-phosphorylated sites (*54*). For the carboxyl-terminal domain of FCP1, it is still not completely clear as to what determines this highly ordered sequence of phosphorylation reactions but the positioning of acidic residue at the $n+3$ position is clearly important. If acidic residues were the only factors used to rank these three sites in order of preference for CK2 phosphorylation (*54*), S944 would probably be considered the preferred site since it has acidic residues at $n+1$ and $n+3$, in addition to acidic residues at $n-4$ and $n+4$. S942 would be the considered the second best site, since this site has an acidic residue at $n+3$ in addition to

acidic residues at $n - 4$, $n - 3$, $n - 2$, $n + 5$, and $n + 6$. S943 would be the least likely site to be phosphorylated by CK2, since it lacks an acidic residue at $n + 3$, but has acidic residues at $n - 4$, $n - 3$, $n + 2$, $n + 4$, and $n + 5$. However, it does appear that acidic residues located on the amino-terminal sides of the three serine residues may be crucial for determining the substrate specificity. If the three acidic amino acids located on the amino-terminal side of the S942−S944 site are removed, the peptide ($FCP1_{941-961}$) is no longer a substrate for CK2 in vitro. Still, it is clear that the presence of an acidic residue at $n + 3$ is an overriding factor and in the case of FCP1, S942 and S944 are excellent sites for CK2 phosphorylation. Although additional CK2 phosphorylation sites are present in $FCP1_{879-961}$, they clearly are not in a position to enhance the binding of FCP1 to RAP74 based on the structure of the $RAP74_{436-517}$/$FCP1_{879-961}$ complex (*37*). Therefore these potential CK2 phosphorylation sites were not investigated further.

An important example of multiple serine phosphorylations by CK2 has been observed in the carboxyl-terminal PEST domain of the transcriptional regulatory protein IκBβ. This domain contains a stretch of seven amino acids consisting of five serine and two aspartic acid residues (^{312}SSSSDSD^{318}). Following UV irradiation, IκBβ is heavily phosphorylated by CK2 at a minimum of three serine residues in the PEST domain and these multiple phosphorylations are critical for IκB control of UV-induced NF-κB activation (*56*). It has been clearly demonstrated that S313 and S315 are two of the three phosphorylation sites and that the initial phosphorylation is essential for the subsequent phosphorylation (*57*). However, there have been no detailed studies conducted to determine if the S313 and S315 sites are phosphorylated in a random fashion or in a highly ordered fashion, but both sites contain an acidic residue in the $n + 3$ position as seen in the carboxyl terminus of FCP1.

Post-translational changes such as phosphorylation can cause dramatic changes in protein conformation or very distinct localized changes in a ligand-binding site. We have demonstrated that both RAP74-binding sites of FCP1 contain conserved CK2 sites that when phosphorylated lead to enhanced binding. The exact biological reason for two RAP74-binding sites in FCP1 is still unknown. The two sites may recruit RAP74 at temporally distinct events within the cell for distinct purposes. The additive effects of multiple phosphorylations within the binding site could serve to strengthen such a macromolecular interaction. The NMR results show that phosphorylation within both the RAP74-binding sites of FCP1 leads to distinct interactions with $RAP74_{436-517}$, most likely involving the formation of ion pairs and/or electrostatic effects. CK2 phosphorylation of FCP1 may provide a selective advantage for binding RAP74 over other potential targets. Interestingly, we have shown in an accompanying paper that Tat can both block CK2 phosphorylation of T584, and inhibit binding of RAP74 to the central domain of FCP1 (*29*). This enhanced binding of FCP1 to RAP74 following phosphorylation is believed to stimulate FCP1 phosphatase activity contributing to CTD dephosphorylation. We have made initial attempts to determine if T584, S942, S943, and S944 are phosphorylated in vivo in human cells (K.L.A., M.B.R., M.J.C., A.G.M., P.L., and J.G.O. Unpublished data). In our preliminary MS studies of FCP1 isolated from human cells, we were not able to identify phosphorylated peptides from the central domain containing T584, or peptides from the carboxyl-terminal domain containing S942−S944 following proteolytic digestion, presumably due to the acidity of these regions in FCP1. It is certainly possible that these sites are not phosphorylated to a significant extent under normal cellular conditions, but may be heavily phosphorylated following special conditions such as stress or DNA damage as is the case with IκB (*56*). Future studies are needed to address the in vivo physiological consequences and possible regulation of FCP1 by CK2 as well as other kinases.

ACKNOWLEDGMENT

We thank Dr. Ettore Appella for synthesis of the $FCP1_{579-600}$ ($T584PO_4$) peptide. We also thank Dr. Claiborne Glover, Dr. Mark Emmett, Dr. Christopher Hendrickson, and Mr. John Quinn for valuable discussions.

REFERENCES

1. Corden, J. L., Cadena, D. L., Ahearn, J. M., and Dahmus, M. E. (1985) A unique structure at the carboxyl terminus of the largest subunit of eukaryotic RNA polymerase II. *Proc. Natl. Acad. Sci. U.S.A. 82*, 7934−7938.
2. Corden, J. L. (1990) Tails of RNA polymerase II. *Trends Biochem. Sci. 15*, 383−387.
3. Bensaude, O., Bonnet, F., Casse, C., Dubois, M. F., Nguyen, V. T., and Palancade, P. (1999) Regulated phosphorylation of the RNA polymerase II C-terminal domain (CTD). *Biochem. Cell Biol. 77*, 249−255.
4. West, M. L., and Corden, J. L. (1995) Construction and analysis of yeast RNA polymerase II CTD deletion and substitution mutations. *Genetics 140*, 1223−1233.
5. Lu, H., Flores, O., Weinmann, R., and Reinberg, D. (1991) The nonphosphorylated form of the RNA polymerase II preferentially associates with the preinitiation complex. *Proc. Natl. Acad. Sci. U.S.A. 88*, 10004−10008.
6. O'Brien, T. S., Hardin, S., Greenleaf, A., and Lis, J. T. (1994) Phosphorylation of RNA polymerase II C-terminal domain and transcriptional elongation. *Nature 370*, 75−77.
7. Proudfoot, N. J., Furger, A., and Dye, M. J. (2002) Integrating mRNA processing with transcription. *Cell 108*, 501−512.
8. Feaver, W. J., Gileadi, O., Li, Y., and Kornberg, R. D. (1991) CTD Kinase associated with yeast RNA polymerase II initiation factor b. *Cell 67*, 1223−1230.
9. Lu, H., Zawel, L., Fisher, L., Egly, J. M., and Reinberg, D. (1992) Human general transcription factor IIH phosphorylates the C-terminal domain of RNA polymerase II. *Nature 358*, 641−645.
10. Serizawa, H. R., Conaway, R. C., and Conaway, J. W. (1992) A carboxyl-terminal-domain kinase associated with RNA polymerase II transcription factor delta from rat. *Proc. Natl. Acad. Sci. U.S.A. 89*, 7476−7480.
11. Liao, S. M., Zhang, J., Jeffery, D. A., Koleske, A. J., Thompson, C. M., Chao, D. M., Viljoen, M., van Huren, H. J., and Young, R. A. (1995) A kinase-cyclin pair in the RNA polymerase II holoenzyme. *Nature 374*, 193−196.
12. Marshall, N. F., Peng, J., Xie, Z., and Price, D. H. (1996) Control of RNA polymerase II elongation potential by a novel carboxyl-terminal domain kinase. *J. Biol. Chem. 271*, 27176−27183.
13. Yeo, M., Lin, P. S., Dahmus, M. E., and Gill, G. N. (2003) A novel RNA polymerase II c-terminal domain phosphatase that preferentially dephosphorylates serine 5. *J. Biol. Chem. 278*, 26078−26085.
14. Chambers, R. S., and Dahmus, M. E. (1994) Purification and characterization of a phosphatase from HeLa cells which dephosphorylates the C-terminal domain of RNA polymerase II. *J. Biol. Chem. 269*, 26243−26248.
15. Archambault, J., Chambers, R. S., Kobor, M. S., Ho, Y., Cartier, M., Bolotin, D., Andrews, B., Kane, C. M., and Greenblatt, J. (1997) An essential component of a C-terminal domain phosphatase that interacts with transcription factor IIF in *Saccharomyces cerevisiae*. *Proc. Natl. Acad. Sci. U.S.A. 94*, 14300−14305.

16. Archambault, J., Pan, G., Dahmus, G. K., Cartier, M., Marshall, N., Zhang, S., Dahmus, M. E., and Greenblatt, J. (1998) FCP1, the RAP74-interacting subunit of a human protein phosphatase that dephosphorylates the carboxy-terminal domain of RNA polymerase IIO. *J. Biol. Chem. 273*, 27593−27601.
17. Chambers, R. S., and Dahmus, M. E. (1996) Purification and characterization of an RNA polymerase II phosphatase from yeast. *J. Biol. Chem. 271*, 24498−24504.
18. Cho, H., Kim, T. K., Mancebo, H., Lane, W. S., Flores, O., and Reinberg, D. (1999) A protein phosphatase functions to recycle RNA polymerase II. *Genes Dev. 13*, 1540−1552.
19. Kobor, M. S., Archambault, J., Lester, W., Holstege, F. C. P., Gileadi, O., Jansma, D. B., Jennings, E. G., Kouyoumdjian, F., Davidson, A. R., Young, R. A., and Greenblatt, J. (1999) An unusual eukaryotic protein phosphatase required for transcription by RNA polymerase II and CTD dephosphorylation in *S. cerevisiae*. *Mol. Cell 4*, 55−62.
20. Schroeder, S. C., Schwer, B., Shuman, S., and Bentley, D. (2000) Dynamic association of capping enzymes with transcribing RNA polymerase II. *Genes Dev. 14*, 2435−2440.
21. Mandal, S. S., Cho, H., Kim, S., Cabane, K., and Reinberg, D. (2002) FCP1, a phosphatase specific for the heptapeptide repeat of the largest subunit of RNA polymerase II, stimulates transcription elongation. *Mol. Cell. Biol. 22*, 7543−7552.
22. Costa, P. J., and Arndt, K. M. (2000) Synthetic lethal interactions suggest a role for the *Saccharomyces cerevisiae* Rtf1 protein in transcription elongation. *Genetics 156*, 535−547.
23. Lindstrom, D. L., and Hartzog, G. A. (2001) Genetic interactions of Spt4-Spt5 and TFIIS with the RNA polymerase II CTD and CTD modifying enzymes in *Saccharomyces cerevisiae*. *Genetics 159*, 487−497.
24. Cho, E.-J., Kobor, M. S., Kim, M., Greenblatt, J., and Buratowski, S. (2001) Opposing effects of Ctk1 kinase and Fcp1 phosphatase at Ser 2 of the RNA polymerase II C-terminal domain. *Genes Dev. 15*, 3319−3329.
25. McCracken, S., Fong, N., Yankulov, K., Bothers, G., Siderovski, D., Hessel, A., Forster, S., Program, A. E., Shuman, S., and Bentley, D. L. (1997) 5′-Capping enzymes are targeted to pre-mRNA by binding to the phosphorylated carboxy-terminal domain of RNA polymerase II. *Genes Dev. 11*, 3306−3318.
26. Cho, E.-J., Takagi, T., Moore, C. R., and Buratowski, S. (1997) mRNA capping enzyme is recruited to the transcription complex by phosphorylation of the RNA polymerase II carboxy-terminal domain. *Genes Dev. 13*, 3319−3326.
27. Licciardo, P., Amente, S., Ruggiero, L., Monti, M., Pucci, P., Lania, L., and Majello, B. (2003) The FCP1 phosphatase interacts with RNA polymerase II and with MEP50 a component of the methylosome complex involved in the assembly of snRNP. *Nucl. Acids Res. 31*, 999−1005.
28. Collet, J. F., Stroobant, V., Pirard, M., Delpierre, G., and Schaftingen, E. V. (1998) A new class of phosphotransferases phosphorylated on an aspartate residue in an amino-terminal DXDX(T/V) motif. *J. Biol. Chem. 273*, 14107−14112.
29. Abbott, K. L., Archambault, J., Xiao, H., Nguyen, B. D., Roeder, R. G., Greenblatt, J., Omichinski, J. G., and Legault, P. Interactions of the HIV-1 Tat and RAP74 proteins with the RNAPII CTD phosphatase FCP1. *Biochemistry 44*, 2716−2731.
30. Marshall, N. F., Dahmus, G. K., and Dahmus, M. E. (1998) Regulation of carboxyl-terminal domain phosphatase by HIV-1 Tat protein. *J. Biol. Chem. 273*, 31726−31730.
31. Chambers, R. S., Wang, B. Q., Burton, Z. F., and Dahmus, M. E. (1995) The activity of COOH-terminal domain phosphatase is regulated by a docking site on RNA polymerase II and by the general transcription factors IIF and IIB. *J. Biol. Chem. 270*, 14962−14969.
32. Licciardo, P., Ruggiero, L., Lania, L., and Majello, B. (2001) Transcription activation by targeted recruitment of the RNA polymerase II CTD phosphatase FCP1. *Nucl. Acids Res. 29*, 3539−3545.
33. Kobor, M. S., Simon, L. D., Omichinski, J., Zhong, G., Archambault, J., and Greenblatt, J. (2000) A motif shared by TFIIF and TFIIB mediates their interaction with the RNA polymerase II carboxy-terminal domain phosphatase Fcp1p in *Saccharomyces cerevisiae*. *Mol. Cell. Biol. 20*, 7438−7449.
34. Nguyen, B. D., Chen, H.-T., Kobor, M. S., Greenblatt, J., Legault, P., and Omichinski, J. G. (2003) Solution structure of the carboxyl-terminal domain of RAP74 and NMR characterization of the FCP1-binding sites of RAP74 and human TFIIB. *Biochemistry 42*, 1460−1469.
35. Friedl, E. M., Lane, W. S., Erdjument-Bromage, H., Tempst, P., and Reinberg, D. (2003) The C-terminal domain phosphatase and transcription elongation activities of FCP1 are regulated by phosphorylation. *Proc. Natl. Acad. Sci. U.S.A. 100*, 2328−2333.
36. Palancade, B., Dubois, M.-F., and Bensaude, O. (2002) FCP1 Phosphorylation by Casein Kinase 2 Enhances Binding to TFIIF and RNA Polymerase II Carboxyl-terminal Domain Phosphatase Activity. *J. Biol. Chem. 277*, 36061−36067.
37. Nguyen, B. D., Abbott, K. L., Potempa, K., Kobor, M. S., Archambault, J., Greenblatt, J., Legault, P., and Omichinski, J. G. (2003) NMR structure of a complex containing the TFIIF subunit RAP74 and the RNA polymerase II carboxyl-terminal domain phosphatase FCP1. *Proc. Natl. Acad. Sci. U.S.A. 100*, 5688−5693.
38. Quinn, J. P., Emmett, M. R., and Marshall, A. G. A device for fabrication of emitters for low-flow electrospray ionization. In *I46th ASMS Conference on Mass Spectrometry and Allied Topics.* 1388, 1998.
39. Hakansson, K., Chalmers, M. J., Quinn, J. P., McFarland, M. A., Hendrickson, C. L., and Marshall, A. G. (2003) Combined electron capture and infrared multiphoton dissociation for multistage MS/MS in a Fourier transform ion cyclotron resonance mass spectrometer. *Anal. Chem 75*, 3256−3262.
40. Senko, M. W., Canterbury, J. D., Guan, S., and Marshall, A. G. (1996) A high-performance modular data system for FT-ICR mass spectrometry. *Rapid Commun. Mass Spectrom. 10*, 1839−1844.
41. Chowdhury, S. K., Katta, V., and Chait, B. T. (1990) An electrospray-ionization mass spectrometer with new features. *Rapid Commun. Mass Spectrom. 4*, 81−87.
42. Wilcox, B. E., Hendrickson, C. L., and Marshall, A. G. (2002) Improved ion extraction from a linear octopole ion trap: SIMION analysis and experimental demonstration. *J. Am. Soc. Mass Spectrom. 13*, 304−1312.
43. Comisarow, M. B., and Marshall, A. G. Frequency-sweep Fourier transform ion cyclotron resonance spectroscopy. *Chem. Phys. Lett. 26*, 489−490 (1974).
44. Marshall, A. G., and Roe, D. C. (1980) Theory of Fourier transform ion cyclotron resonance mass spectroscopy: Response to frequency-sweep excitation. *J. Chem. Phys. 73*, 1581−1590.
45. Marshall, A. G., and Verdun, F. R. (1990) *Fourier Transforms in NMR, Optical, and Mass Spectrometry: A User's Handbook*, Elsevier, Amsterdam.
46. Ledford, E. B., Jr., Rempel, D. L., and Gross, M. L. (1984) Space charge effects in Fourier transform mass spectrometry: Mass Calibration. *Anal. Chem. 56*, 2744−2748.
47. Hendrickson, C. L., Quinn, J. P., Emmett, M. R., and Marshall, A. G. (2000) Quadrupole mass filtered external accumulation for Fourier transform ion cyclotron resonance mass spectrometry. *In 48th ASMS Conference on Mass Spectrometry and Allied Topics*, Long Beach, CA.
48. Marshall, A. G., Wang, T.-C. L., and Ricca, T. L. (1985) Tailored excitation for Fourier transform ion cyclotron resonance mass spectrometry. *J. Am. Chem. Soc. 107*, 7893−7897.
49. Guan, S., and Marshall, A. G. (1996) Stored waveform inverse Fourier transform (SWIFT) ion excitation in trapped-ion mass spectrometry: Theory and applications. *Int. J. Mass Spectrom. Ion Processes 157/158*, 5−37.
50. Shen, J., Smith, R. A., Stoll, V. S., Edalji., R., Jakob, C., Walter, K., Gramling, E., Dorwin, S., Bartley, D., Gunasekera, A., Yang, J., Holzman, T., and Johnson, R. W. (2004) Characterization of protein kinase A phosphorylation: multi-technique approach to phosphate mapping. *Anal. Biochem. 324*, 204−218.
51. Kay, L. E., Keifer, P., and Saarinen, T. (1992) Pure absorption gradient enhanced heteronuclear single quantum correlation spectroscopy with improved sensitivity. *J. Am. Chem. Soc. 114*, 10663−10665.
52. Delaglio, F., Grzesiek, S., Vuister, G. W., Zhu, G., Pfeifer, J., and Bax, A. (1995) NMRPipe: a multidimensional spectral processing system based on UNIX pipes. *J. Biomol. NMR 6*, 277−293.
53. Koradi, R., Billeter, M., and Wüthrich, K. (1996) MOLMOL: a program for display and analysis of macromolecular structures. *J. Mol. Graphics 14*, 51−55.
54. Meggio, F., and Pinna, L. A. (2003) One-thousand-and-one substrates of protein kinase CK2? *FASEB J. 17*, 349−368.
55. Jaffe, H., Veeranna, H., and Pant, H. C. (1998) Characterization of serine and threonine phosphorylation sites in beta-elimination/

ethanethiol addition-modified proteins by electrospray tandem mass spectrometry and database searching. *Biochemistry 37*, 16211−16224.

56. Kato, T. J., Delhase, M., Hoffmann, A., and Karin, M. (2003) CK2 is a C-terminal IκB kinase responsible for NF-κB activation during the UV response. *Mol. Cell 1*, 829−839.

57. McKinsey, T. A., Zhi-Liang, C., and Balard, D. W. (1997) Phosphorylation of the PEST domain of IκBβ regulates the function of NF-κB/IκBβ complexes. *J. Biol. Chem. 272*, 22377−22380.

BI047958H